

Barrier Properties for Short-Fiber-Reinforced Epoxy Foams

M. V. Alonso,^{1*} M. L. Auad,¹ U. Sorathia,² N. E. Marcovich,³ S. R. Nutt¹

¹Materials Science Department, Gill Foundation Composites Center, University of Southern California, Los Angeles, California 90089-0241

²Carderock Division, Naval Surface Warfare Center, West Bethesda, Maryland 20817-5700

³Institute of Research in Materials Science and Technology, Univ. Nacional de Mar del Plata, CONICET, Juan B. Justo 4302, 7600 Mar del Plata, Argentina

Received 6 February 2006; accepted 20 April 2006

DOI 10.1002/app.24693

Published online in Wiley InterScience (www.interscience.wiley.com).

ABSTRACT: The barrier properties of short-fiber-reinforced epoxy foam are characterized and compared with unreinforced epoxy foam in terms of moisture absorption, flammability properties, and impact properties. Compression and shear properties are also included to place in perspective the mechanical behavior of these materials. Compared with conventional epoxy foam, foam reinforced with aramid fibers exhibits higher moisture absorption and

lower diffusion, while glass-fiber-reinforced foam is significantly stiffer and stronger. In addition, the polymeric foam composites studied present superior fire-resistance compared with conventional epoxy foam systems. © 2006 Wiley Periodicals, Inc. *J Appl Polym Sci* 102: 3266–3272, 2006

Key words: foams; fibers; fire resistance; mechanical properties; moisture

INTRODUCTION

Epoxy resins are high-performance thermosetting polymers widely used in adhesives, flooring and paving applications, molding products, and composites. The performance of epoxy resins is often enhanced by the addition of fillers such as particles (e.g., microspheres) or/and different types of fibers (e.g., glass, carbon, aramid). The latter materials—epoxy composites—merit special attention because they are lightweight structural materials that exhibit excellent mechanical performance and attractive dielectric properties.^{1,2} They are used in a broad range of applications in the construction, transportation, marine, and aerospace industries.^{3–5}

Epoxy foams can also be reinforced with fibers. The extremely low density of foam structures, coupled with the intrinsic strength and adhesion of epoxy and high-performance fibers, yields an ultralight structural material that is strong, durable, and damage-tolerant.^{6,7} Such materials constitute a low-cost alternative to costly honeycomb core materials commonly used in sandwich structures.

While mechanical performance is critical to the design of reinforced epoxy composites, other factors

can be equally important. For example, humidity exposure and resulting water absorption can reduce fiber adhesion in the material, producing deleterious effects on mechanical performance and adding unwanted weight. Another concern for most aircraft and marine applications is the fire resistance of composites, which can affect mechanical performance and more importantly, diminish human safety.

In this article, we examine the influence of glass and aramid fibers on mechanical properties, water absorption, and fire resistance of epoxy foams, and compare the results with unreinforced foams. The influence of different loadings and fiber types on foam properties is also analyzed. The samples are characterized using compression, shear, and impact tests, as well as water absorption and flammability, smoke density, and toxicity (FST) tests.

EXPERIMENTAL

Materials and synthesis of composite foams

Epoxy foams were formulated using a commercial system consisting of epoxy, amino hardener, and polydimethylsiloxane as chemical foaming agent (REN 1774, Ciba-Geigy). The epoxy foam was synthesized with a weight ratio of epoxy : hardener : blowing agent of 100 : 25 : 2.4. Short aramid fibers were utilized (Nomex[®], DuPont) with chop length of 6.3 mm and an average diameter of 15 μm . Glass fibers (Owens

*Present address: Departamento de Ingeniería Química, Facultad de Ciencias Químicas, Universidad Complutense de Madrid, Avda de la Complutense s/n, 28040 Madrid, Spain.

Correspondence to: M. V. Alonso (valonso@quim.ucm.es).

Corning) were also used, with chop length of 6.3 mm and an average diameter of 17 μm .

The synthesis of reinforced epoxy foams was carried out blending the fibers with the resin in a high-speed, dual-axis mixer (Keyence HM-101). The fibers were dispersed in the epoxy resin using the mixer. After this stage, hardener and siloxane were added [full details appear in Ref. 6]. The sample was poured into a mold and maintained at room temperature for 24 h. The sample was postcured for 2 h at 100°C. All foams were manufactured to achieve a density of 300 kg/m³ (or \sim 18.5 pcf).

Mechanical testing

Compression testing was performed using a universal testing machine (INSTRON 8531) in accordance with ASTM D1621. Specimens were cut with a diamond blade band saw and polished to a size of 30 \times 30 \times 25.4 mm³. Samples were compressed between two stainless steel platens using a crosshead rate of 2.5 mm/min. From the stress–strain curve, the compressive modulus was determined using the steepest initial slope, and the strength was calculated from the maximum load.

Shear testing was performed according to ASTM C273. Sample dimensions were 25.4 \times 6.4 \times 30.4 mm³. The polished samples were bonded to stainless steel plates using a fast-cure epoxy adhesive. The shear modulus and strength were calculated from the

stress–strain curve according to ASTM standard procedures.

Instrumented falling weight impact (IFWI) tests were performed using a falling weight impact tower (Fractovis Ceast). The plaques, clamped on a supporting ring of 40 mm diameter, were impacted with a hemispherically tipped dart at an incident speed of 3.33 m/s. An impactor mass of 18.49 kg was used, and the response of load was recorded for 32 m/s. At least four plates for each material were impacted.

Moisture absorption tests

Sample dimensions of 5 \times 50 \times 50 mm³ long were used for moisture absorption tests, in accordance with ASTM D5229, which specifies a nominal-length-of-one-side to thickness ratio of 10 : 1. The samples were dried in a vacuum oven at 60°C until no weight change was observed. Dried specimens were placed in an environmental chamber maintained at 80% relative humidity and room temperature. The weight of the samples was monitored until specimens reached equilibrium conditions.

FST tests

FST tests were performed on composite foams using a cone calorimeter, in accordance with ASTM E1354. Sample dimensions were 6.4 \times 100 \times 100 mm³ (4 \times 4 in.), as shown in Figure 1. In fire tests, the

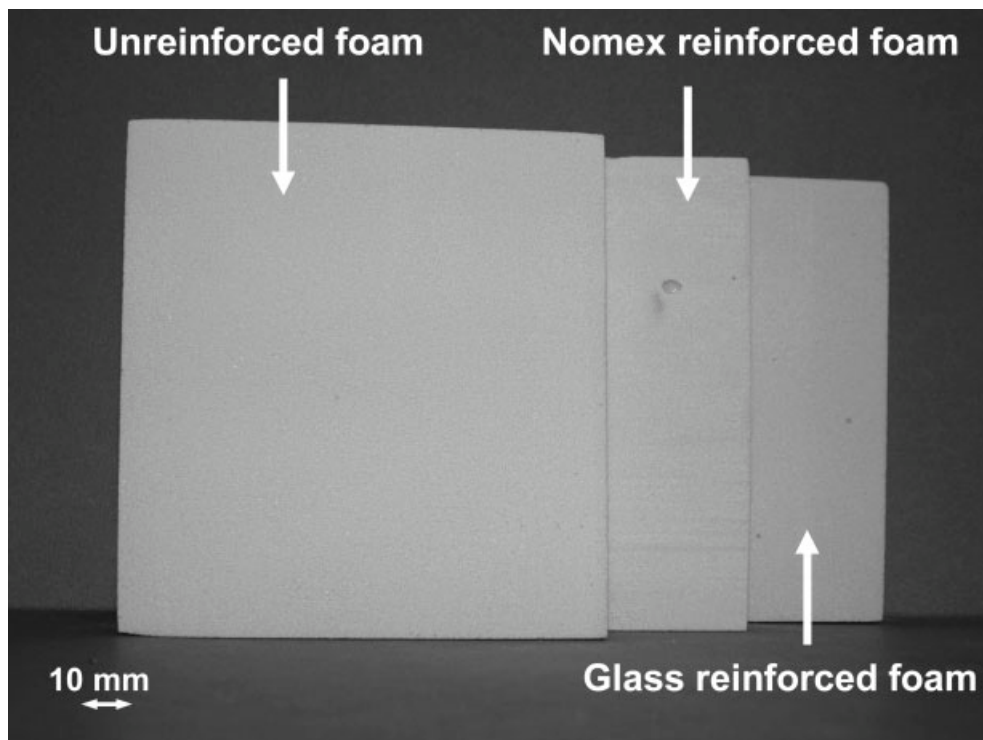


Figure 1 Original shape of unreinforced and short-fiber-reinforced epoxy foams before FST tests.

broad specimen surface was exposed to the electric radiant heat source in the calorimeter. Composite samples were exposed to an incident heat flux of 50 kW/m² generated by the heat source for times up to 30 min. The heat flux was selected to approximate the heat intensity from a medium-sized room fire. The ignitability, peak heat release rate, the evolution of CO, and the time to sustained ignition were measured.

RESULTS AND DISCUSSION

Mechanical properties

The results of compression and shear tests on the different reinforced foams are summarized in Table I.⁶ In general, glass-reinforced epoxy foams exhibit higher compressive modulus values than aramid-reinforced foams because of the higher bending stiffness of glass fibers. However, aramid-reinforced foams exhibit larger increases in compressive strength, a phenomenon attributed to micro-peel phenomenon in the fibers.⁹ With respect to shear properties, the reinforced foams exhibit significant enhancements (20–140%) in both modulus and strength. Note that the strain energy density of the foam composite with 5 wt % aramid fibers shows a 4-fold increase relative to the unreinforced foam. The strain energy density is an important indicator of energy absorption and fracture resistance.

While compressive and shear properties are undoubtedly critical factors for core materials in sandwich structures, impact resistance is important for durability and damage tolerance of foams. The IFWI technique is widely accepted for assessment of out-of-plane fracture response of plastics and composites. This method provides an accurate measure of the material response against impact loads parallel to the thickness direction. From the IFWI fractograms, the following parameters were determined by data reduction:

- The maximum strength (σ_d). The maximum load registered (F_{\max}) in the fractogram can be converted to a stress, which represents the impact bending strength at crack initiation:

$$\sigma_d = \frac{2.5 F_{\max}}{l^2} \quad (1)$$

where l is the sample thickness.

- The energy at crack initiation, which can be normalized by thickness:

$$E_i = \frac{1}{l} \int_0^{X_{\max}} F dX \quad (2)$$

where X is the displacement.

- The total energy required to penetrate the specimen completely, normalized by thickness:

$$E_t = \frac{1}{l} \int_0^{X_{\text{total}}} F dX \quad (3)$$

- The ductile failure mode can be described by the ductility index (DI). A DI = 0 indicates that the sample is fully brittle and a DI = 1 that the failure is fully ductile.¹⁰

$$DI = \frac{E_t - E_i}{E_t} = \frac{E_p}{E_t} \quad (4)$$

where E_p is the energy required to complete disk penetration (propagation energy). The equations above were first derived by Jones et al.,¹¹ and now are commonly used in works describing mechanical behavior of foams.^{12–14}

The measured values of maximum load (F_{\max}), maximum energy (E_{\max}), total energy (E_{total}), and total time (t_{total}) for the composite foams studied are sum-

TABLE I
Compressive (Parallel^a) and Shear Properties (Perpendicular^b) of Foams
with a Length of 6.3 mm Fiber (Density = 300 kg/m³)

Foam formulation	Compressive properties		Shear properties		
	Modulus (MPa)	Strength (MPa)	Modulus (MPa)	Strength (MPa)	Strain energy density (J) (10 ⁻⁶ /m ³)
Unreinforced	73.69	2.66	386.83	10.49	14.47
2.5% Aramid reinforced	62.72	2.62	503.67	17.23	31.04
5% Aramid reinforced	92.49	3.21	551.04	24.45	57.06
2.5% Glass reinforced	85.93	2.78	489.48	12.11	16.20
5% Glass reinforced	116.64	2.86	439.54	14.88	23.31
Phenolic ^c	36.5	0.4	12.3	0.30	–
Polyurethane ^c	183.29	4.25	32.39	2.82	–

^a Loading direction with respect to the 2 foam rise direction.

^b 'Perpendicular' means the shear plane is perpendicular to the foaming direction.

^c Data from the manufacturer's datasheets.⁸

marized in Table II. Note that the maximum load for epoxy foam with 5 wt % glass fiber is slightly lower than the unreinforced counterpart, while the foam containing only 2.5 wt % glass fiber showed increases in maximum load and energy of 23 and 16%, respectively. Similarly, the foam with 5 wt % aramid fiber showed only a modest increase in maximum load point ($\sim 5\%$), while the foam 2.5 wt % aramid fibers showed an increase in maximum load of 20% relative to the unreinforced foam. Thus, while glass fibers were more effective than aramid fibers in enhancing impact properties, higher fiber loadings caused a decrease in impact properties relative to the unreinforced foam. At lower fiber loadings, fibers increase the resistance to impact damage, presumably by bridging cracks and by pullout. However, at higher loadings, fibers facilitate impact damage, a phenomenon that might be related to inadequate fiber dispersion. The initiation of fracture during impact loading of unreinforced foam is caused mainly by craze formation,¹⁵ while in composite foams, additional mechanisms are activated, such as pullout, deflection, and debonding. The effects of the high loading rates on fracture mechanisms in composite foams is presently not well understood, and will require further study.

Moisture absorption

Presentation and discussion of the moisture absorption data requires a brief description of the theory of moisture diffusion in polymeric materials. More detailed descriptions are provided elsewhere.¹⁶⁻¹⁸ The mechanism of moisture diffusion can be described by Fick's second law with a diffusivity constant (D), which normally represents nonsteady state diffusion in a polymer in three dimensions such as follows:

$$\frac{M_t}{M_\infty} = 1 - \sum_0^{\infty} \frac{8}{(2n+1)^2 \pi^2} \exp\left[\frac{-D\pi^2}{4l^2} (2n+1)^2 t\right] \quad (5)$$

In our work, one-dimensional diffusion through a sample of thickness $2l$ was measured, and thus the relative moisture uptake was approximated by the following expression (where only the terms for $n = 0$ appear):

TABLE II
Impact Properties of Foams with a Length of 6.3 mm
Fiber (Density = 300 kg/m³)

Foam formulation	F_{\max} (N)	E_{\max} (J)	E_{total} (J)	t_{total} (ms)
Unreinforced	2309.75	20.80	42.47	12.68
2.5% aramid reinforced	2836.62	19.39	39.06	11.37
5% aramid reinforced	2426.99	13.11	35.31	12.63
2.5% glass reinforced	2993.64	24.86	53.05	13.06
5% glass reinforced	2211.95	12.94	33.78	10.01

$$\frac{M_t}{M_\infty} = 1 - \frac{8}{\pi^2} \exp\left[\frac{-D\pi^2}{4l^2} t\right] \quad (6)$$

where M_t is the weight gained at time t , and M_∞ is the maximum weight gained at the equilibrium state. An expression similar to eq. (5) was used to predict the moisture content,^{17,18} given by:

$$\frac{M_t}{M_\infty} = 1 - \exp\left[-7.3 \cdot \left(\frac{Dt}{4l^2}\right)^{0.75}\right] \quad (7)$$

Fick's second law is based on a linear relationship between the moisture gain (M_t/M_∞) and time ($t^{1/2}$). Consequently, the diffusivity coefficient can be determined from the resultant slope of the following equation^{7,16} for small values of times ($M_\infty/M_t \leq 0.5$).

$$\frac{M_t}{M_\infty} = 4 \cdot \left(\frac{Dt}{\pi 4l^2}\right)^{0.5} \quad (8)$$

On the other hand, in an ideal, void-free composite, the process of diffusion will depend primarily on:^{19,20}

- The diffusivity of the continuous matrix, D_m and that of the reinforcement, D_f .
- The volume concentration of the matrix ($1 - V_f$) and the filler V_f and
- The spatial distribution and orientation of the fibers in the matrix (in the case of fiber reinforcement).

In the last case, the effective conductivity, D_c , of the composite will also depend on the dimensions of the fibers and the degree of anisotropy of the relevant properties of the fibers and matrix materials. Furthermore, because the composites prepared in this work are foams, they are not void-free and thus, the effective diffusivity also depends on void concentration. Moreover, the effective diffusion coefficients used throughout this article may include non-Fickian effects present in the system (e.g., capillary transfer of moisture and water diffusion through the microscopic and submicroscopic structure of the foams).

Typical plots of percentage weight gain as a function of root time for epoxy foams with different fiber contents are shown in Figure 2. The moisture absorption behavior is well-fitted in M_∞ [eq. (7)] for all foams tested. On the other hand, the nonsteady-state moisture absorption of the specimens is also well-described by this model. However, data from epoxy foams do not conform to the steady-state predictions because of the morphological features of this material,¹⁸ which presents preferred pathways for diffusion of water molecules.

Glass-fiber reinforced epoxy foams reach moisture saturation after about 2.5 days, independent of fiber

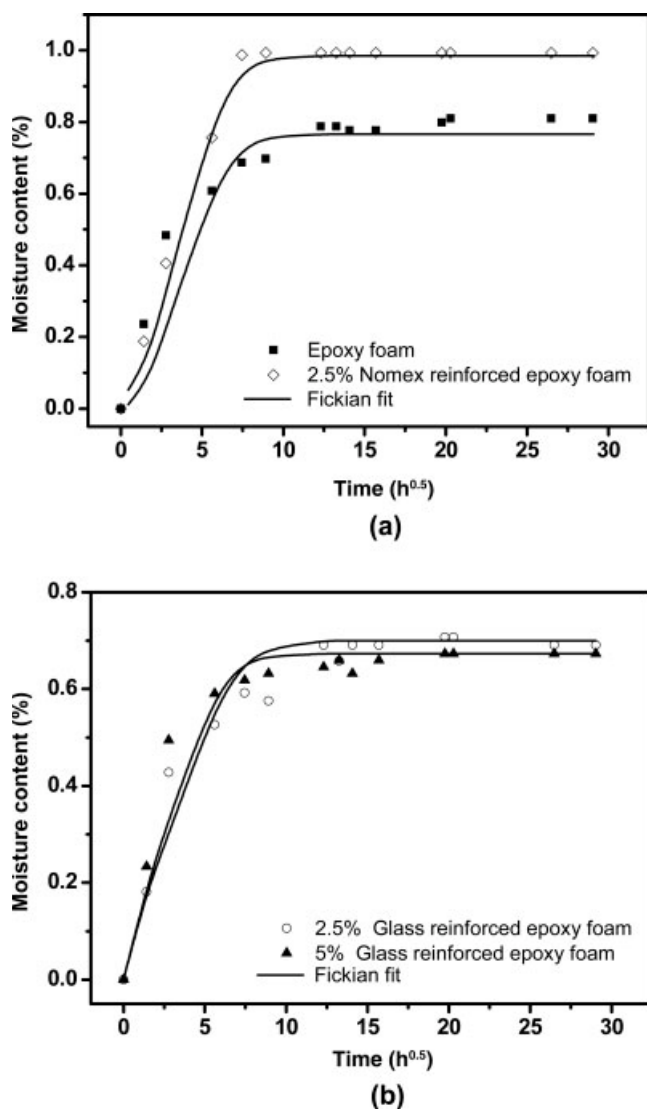


Figure 2 Plots of weight gain versus square root time, for (a) epoxy foam and aramid reinforced epoxy foam and (b) glass reinforced epoxy foams.

loading [Fig. 2(a)]. The unreinforced epoxy foam required ~ 6 days and reinforced epoxy foam with 2.5 wt % aramid-fiber required ~ 8 days to achieve moisture saturation. The moisture absorption rates for glass-reinforced epoxy foams were greater than that of unreinforced and aramid-reinforced epoxy foams. However, epoxy foam with 2.5 wt % aramid fiber exhibited a higher moisture content after reaching the equilibrium state [Fig. 2(b)]. In general, the saturated humidity content of the composite foams is predicted by the model.

The effective diffusivity values predicted by Fick's second law for the epoxy foams are displayed in Figure 3. A remarkable $\sim 22\%$ reduction in effective diffusivity relative to the unreinforced epoxy foam was achieved with addition of 2.5 wt % glass fiber. In general, the effective diffusivity decreased with increasing fiber content because moisture absorption

of reinforced composites presents complex phenomena. Thus, the effective diffusivity for glass-reinforced epoxy foam is influenced by crosslinking and the cell size reduction that results from glass fiber additions. Note that epoxy foam with 2.5 wt % aramid fiber exhibits a 5% increase in effective diffusivity with respect to unreinforced epoxy foam because of the hydrophilic character of the fibers. In contrast, the addition of 2.5% glass fibers causes a reduction in effective diffusivity, reflecting the hydrophilic behavior of the glass fibers in the foam. Epoxy foam with 5 wt % glass fiber exhibits a diffusivity that is 25% greater than epoxy foam with 2.5% glass fiber (but similar to the diffusivity in 2.5 wt % aramid-reinforced epoxy foam). An increase in the glass fiber loading provides more pathways for accelerated diffusion of water molecules in the foam, which also reduces the adhesion between glass fibers and the matrix. Note that excessive moisture uptake in epoxy foams is expected to adversely affect corrosion processes and degrade thermomechanical properties,^{21,22} factors that are particularly important in electronic applications for foams.

Fire resistance

The burning behavior of reinforced epoxy foams was studied by cone calorimetry, and the flammability properties are shown in Table III. The time to ignition (TTI) for the composite foams was low relative to phenolic laminates, which typically show TTIs of 170 s.²³ This finding was not unexpected, because flammability properties of phenolic compounds are generally far superior to those of epoxy systems. However, the composite foams were formulated with epoxy REN 1774, which exhibits a delay in TTI of $\sim 20\%$ relative to epoxy Epon826 (Table III). Note that the epoxy resin used contains proprietary fire-retardant additives to improve FST properties.

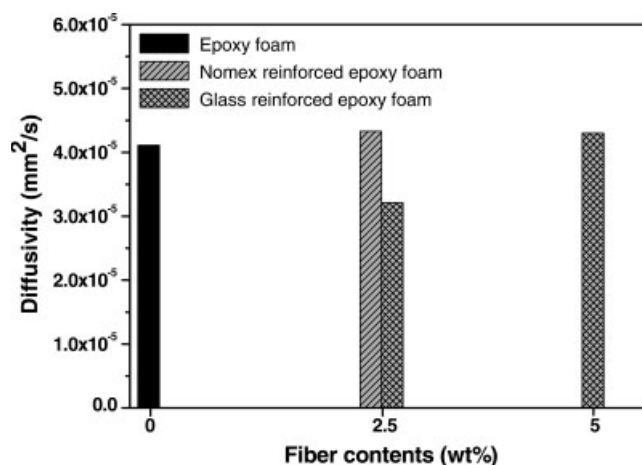


Figure 3 Evolution of moisture diffusivity as a function of fiber contents for epoxy foams.

TABLE III
Cone Calorimetric Results for Unreinforced and Reinforced Foams at 50 kW/m²

Foam formulation	TTI (s)	Peak HRR (kW/m ²)	HRR 300 s Avg. (kW/m ²)	Total HR (MJ/m ²)	Weight loss (%)	Avg. CO (kg/kg)	Avg. CO ₂ (kg/kg)	Avg. CO/CO ₂ (kg/kg)
Unreinforced (REN 1774)	9	305	203	106	65.7	0.037	1.815	0.020
2.5% aramid reinforced	11	318	217	136	66.6	0.041	1.766	0.023
2.5% glass reinforced	9	265	129	147	62	0.015	1.192	0.013
Phenolic laminates ^a	170	100	–	206	23	–	–	–
Epoxy foam (Epon826) ^b	2.3	314	195	–	67	–	–	0.023

^a Ref. 23.

^b Ref. 24.

The heat release rate (HRR) curves for the composite foams show an initial peak at about 1 min (Fig. 4), which is attributed to fiber and matrix decomposition near the heated surface.²⁵ The second large peak is caused by matrix decomposition (unreinforced epoxy foam) and fiber decomposition (reinforced epoxy foams). The foam reinforced with 2.5 wt % glass fiber displayed a lower average HRR than the unreinforced foam. However, phenolic foams exhibit much greater fire resistance and much lower total heat release (THR). The weight loss of the different epoxy foams, in general, show similar values, which indicates good fiber–matrix adhesion. Finally, the average CO/CO₂ yield value for the foam with 2.5% glass decreased by 35 and 43% with respect to the unreinforced epoxy foams (REN 1774 and Epon826), respectively. These reductions indicate decreased toxicity as a result of the glass fiber additions.

CONCLUSIONS

Epoxy composite foams reinforced with 2.5 wt % aramid or glass fibers exhibit superior impact properties relative to unreinforced and 5 wt % fiber reinforced epoxy foams. Glass fiber (2.5 wt %) additions reduce both moisture absorption and effective diffusivity in

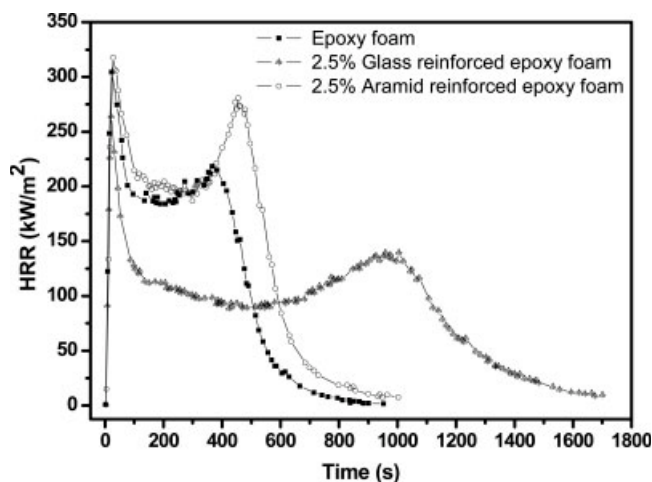


Figure 4 Typical HRR curves for unreinforced and reinforced epoxy foams.

the reinforced composite foam. This may translate into improved corrosion resistance for such materials, an important consideration for electronic applications. The addition of glass fibers improves fire resistance, reducing both CO and CO₂ emissions during combustion of reinforced foam. However, the TTI of the reinforced epoxy foams are relatively short, particularly when compared with phenolic foams.

Several issues require further investigation, including more extensive characterization of mechanical and physical properties, the effects of moisture on thermomechanical properties, and the effects of new additives in the epoxy resin for improving the overall FST fire properties of composite foams.

NOMENCLATURE

D	diffusivity constant
DI	ductility index
E_i	energy at crack initiation
E_p	propagation energy
E_{total}	total energy
F_{max}	maximum load
HRR	average heat release rate
M_t	weight gained at time t
M_{∞}	maximum weight gained at the equilibrium state
t_{total}	total time
TTI	time to ignition
X	displacement

Greek letters

ρ	density
σ_d	maximum strength

The authors gratefully acknowledge the support of the Merwyn C. Gill Foundation. One of the authors, M.V. Alonso, gratefully acknowledges the support of "Secretaría de Estado de Educación y Universidades" (from Spanish Government) and the cosupport of "Fondo Social Europeo."

References

- Komai, K.; Minoshima, K.; Tanaka, K.; Tokura, T. *Int J Fatigue* 2002, 24, 339.
- Kawaguchi, T.; Pearson, R. A. *Polymer* 2003, 44, 4229.

3. Moser, A.; Kamps, E. Lverarbeitung und Anwendungen mit expandierenden EP-Harzen als Matrixsysteme. Presented at the 21st AVK Conference, Mainz, 1987; p 32.
4. Moser, A. Ex-amdoeremde E-pxod-Laminiersysteme. In Conference Verbundwerk'90, Wiesbaden, 1990; p 5.1.
5. Cole, L. F. Concrete Repair Bull 2000, 4, 8.
6. Alonso, M. V.; Auad, M. L.; Nutt, S. Compos A, to appear.
7. Alonso, M. V.; Auad, M. L.; Nutt, S. Compos Sci Technol 2006, 66, 2126.
8. FR-4500[®] Series foam product, General Plastics Manufacturing Company, 2004; Alucopan[®] foam product, Alcan Aires AG Company, 2003.
9. Shen, H.; Nutt, S. Compos A 2003, 34, 899.
10. Trantina, G. G. ASM Handbook, Vol. 20; ASM International: Materials Park, OH; 1997; p 639.
11. Jones, D. P.; Leach, D. C.; Moore, D. R. Plast Rubber Process Appl 1986, 6, 67.
12. Karger-Kocsis, J.; Mouzakis, D. E.; Ehrenstein, G. W.; Varga, J. J Appl Polym Sci 1999, 73, 1205.
13. Mouzakis, D. E.; Harmia, T.; Karger-Kocsis, J. Polym Polym Compos 2000, 8, 167.
14. Acha, B. A.; Reboredo, M. M.; Marcovich, N. E. Polym Int 2006, 55, 1104.
15. Lazzeri, A.; Bucknall, C. B. J Mater Sci 1993, 28, 6799.
16. Crank, J. The Mathematics of Diffusion; Oxford University Press: London, 1970; Chapter IV.
17. Shen, C. H.; Springer, G. S. J Compos Mater 1976, 10, 2.
18. Kim, J.-K.; Hu, C.; Woo, R. S. C.; Sham, M.-L. Compos Sci Technol 2005, 65, 805.
19. Manson, J. A.; Sperling, L. H. Polymer Blends and Composites, 3rd ed.; Premium Press: New York, 1981; Chapter 12.
20. Marcovich, N. E.; Reboredo, M. M.; Aranguren, M. I. Polymer 1999, 40, 7313.
21. Lekatow, A.; Faidi, S. E.; Ghidaoui, D.; Lyon, S. B.; Newman, R. C. Compos A 1997, 28, 223.
22. Luo, S. J.; Lwlawn, J.; Wong, C. P. J Appl Polym Sci 2002, 85, 1.
23. Auad, M. L.; Zhao, L.; Nutt, S.; Sorathia, U. Presented at SAMPE Conference 2004, Long Beach, CA, May 16-20, 2004.
24. Shen, H. Toughening of Phenolic Foam. USC Dissertation Services, 2003.
25. Mouritz, A. P.; Mathys, Z.; Gibson, A. G. Compos A 2006, 37, 1040.